

TLR3 deficiency impairs spinal cord synaptic transmission, central sensitization, and pruritus in mice

Tong Liu, Temugin Berta, Zhen-Zhong Xu, Chul-Kyu Park, Ling Zhang, Ning Lü, Qin Liu, Yang Liu, Yong-Jing Gao, Yen-Chin Liu, Qiufu Ma, Xinzhong Dong, and Ru-Rong Ji

Inventory of supplementary materials submitted:

I. Supplemental Methods and References

II. Supplementary Tables (3)

III. Supplementary Figures (10)

Supplemental Methods

Mice

We used adult mice (25-32 g) for behavioral and histochemical studies. *Tlr3* knockout mice (*Tlr3*^{-/-}; B6;129S1-Tlr3tm1Flv/J) and wild-type mice of the same genetic background (B6129SF1/J) were purchased from the Jackson Laboratories. A targeting vector containing a *loxP* site flanked neomycin resistance cassette and a herpes simplex virus thymidine kinase gene was used to disrupt exon 1. The construct was electroporated into 129S1/Sv-*p*⁺ *Tyr*⁺ *Kitl*^{Sl-J} derived W9.5 embryonic stem (ES) cells. Correctly targeted ES cells were injected into C57BL/6 blastocysts, and the resulting chimeric male mice were crossed to female C57BL/6 mice. Heterozygotes were intercrossed to generate homozygotes. Homozygous mice are viable, fertile, have normal in size and, and display no gross physical or behavioral abnormalities (1). We also obtained *Tlr7*^{-/-} (B6.129S1-Tlr7tm1Flv/J) mice, *Trpv1*^{-/-} mice, and their wild-type (C57BL/6J) control mice from Jackson Laboratories. Male CD1 mice (25-32 g, Charles River) were also used for some behavioral and pharmacological studies. Mice were housed 5 per cage and maintained at Harvard Thorn Building Animal Facility, with identical conditions of temperature (21±1 °C) and humidity (60%±5%) and a 12-hour light/12 hour dark cycle, and were allowed food ad libitum.

Drugs and administration

We purchased histamine, compound 48/80, trypsin, chloroquine, serotonin, and TLR3 agonist polyribo-inosinic/cytidylic acid (PIC) from Sigma-Aldrich, histamine H1 receptor agonist histamine-trifluoromethyl-toluidine (HTMT), capsaicin, and the H4R-selective agonist 4-methylhistamine (4-MeHA) from Tocris, and endothelin-1 (ET-1) from ALEXIS Biochemicals. We also purchased the PAR2 agonist H-Ser-Leu-Ile-Gly-Arg-Leu-NH₂ (SLIGRL-NH₂) and the gastrin-releasing peptide fragment (GRP₁₈₋₂₇) from Bachem. We injected pruritic agents intradermally in the nape of the neck (50 µl) or cheek (10 µl), respectively. Please see more details in the behavioral test session.

We also injected the following reagents intrathecally to target DRG and spinal cord cells. The TRIF peptide inhibitor and control peptide were from Invivogen. The antisense oligodeoxynucleotides (AS-ODN; 5'-AACAAATTGCTTCAAGTCC-3') targeting TLR3 and the control mismatch ODN (MM-ODN; 5'-ACTACTACACTAGACTAC-3') were synthesized by Invitrogen according to the published sequences (2). AS-ODN (10 µg) or MM-ODN (10 µg) were intrathecally injected once a day for 5 days. Selective siRNA targeting TLR3 (5'-GAAGAGGAAUGUUUAAAUCUU-3') and non-targeting control siRNA were synthesized by Dharmacon. siRNA was dissolved in RNase-free water at the concentration of 1 µg/µl as stock solution, and mixed with polyethyleneimine (PEI, Fermentas), 10 min before injection, to increase cell membrane penetration and reduce the degradation. PEI was dissolved in 5% glucose, and 1 µg of siRNA was mixed with 0.18 µl of PEI (3). We intrathecally injected 10 µl of siRNA (3 µg) once a day for 3 days to knockdown TLR3 expression. Capsaicin was dissolved in 10% DMSO. Other reagents were dissolved in sterile saline if not specified. Intrathecal injection was performed by a lumbar puncture to deliver reagent into cerebral spinal fluid. A successful spinal puncture was evidenced by a brisk tail-flick after the needle entry into subarachnoid space (4).

Behavioral testing for itch

Acute injection models. Mice were habituated to the testing environment daily for at least two days before analysis. Mice were shaved at the back of the neck the day before injection. We put mice in small plastic chambers (14 × 18 × 12 cm) on an elevated metal mesh floor and allowed 30 min for habituation before examination. We injected 50 µl of pruritic agent intradermally in the nape of the neck and counted the number of scratches every 5 min for 30 min after the injection. A scratch was counted when a mouse lifted its hindpaw to scratch the shaved region and returned the paw to the floor or to the mouth for licking. On the basis of the previous reports (5, 6) and our recent study (7), we chose the following doses for pruritic agents: 25 ng for ET-1, 20 µg for 5-HT, 100 µg for HTMT, compound 48/80, and SLIGRL-NH₂, 200 µg for chloroquine, 300 µg for trypsin, and 500 µg for histamine and 4-MeHA. We also injected diluted formalin (0.6%, 50 µl) in the nape to induce scratching behaviors. The experimenters were blinded to the genotypes of the animals.

Cheek model. To distinguish itch and pain responses simultaneously, we used the cheek model by injection of chemical into the cheek of mouse (8, 9). After brief anesthesia with isoflurane, we shaved mice on cheeks (approx. 5×8 mm area) two days before experiments. On the day of experiment, we injected 10 µl of reagent (50 µg compound 48/80 or 100 µg chloroquine) into the cheek and counted the number of wipes and the number of scratches for 30 min. We only counted those unilateral wipes with the forelimb that were not part of grooming behavior. One scratch was defined as a lifting of the hind paw toward the injection site on the cheek and then returning the paw to the floor or to the mouth.

Dry skin-induced itch model. We produced a dry skin model to induce chronic itch, as described previously (10, 11), by painting the neck skin with acetone and diethylether (1:1) following by water (AEW) twice a day for 7 days. We examined spontaneous itch by counting the number of scratches for 60 min on day 8 and 9.

Behavioral testing for pain

We habituated animals to the testing environment daily for at least two days before baseline testing. All the behavioral experiments were done by individuals that were blinded to the treatment or genotypes of the mice.

von Frey test. We put mice in boxes on an elevated metal mesh floor and stimulated hindpaw with a series of von Frey hairs with logarithmically incrementing stiffness (0.02-2.56 grams, Stoelting), presented perpendicular to the plantar surface, and determined the 50% paw withdrawal threshold using up-down method (12).

Randall-Selitto test. We used Randall-Selitto Analgesy-meter (Ugo basile, Italy) to examine mechanical sensitivity by applying ascending pressure to the tail of a mouse and determined the mechanical pain threshold when animal showed a clear sign of discomfort or escape, with a cutoff threshold of 250 g to avoid tissue damage (13).

Hargreaves test. For testing heat sensitivity, we put mice in plastic boxes and measured the hindpaw withdrawal latency to Hargreaves radiate heat apparatus (IITC Life Science). We set a cutoff of 20 s to prevent potential tissue damage (14).

Tail immersion test. We used tail immersion test to assess heat pain sensitivity by keeping the tail of a mouse in hot water at 48, 50, or 52 °C and recorded the tail flick latency, with a cutoff time of 10 seconds as previous described (15).

Capsaicin test. Capsaicin (1 and 10 µg in 20 µl 2.5% DMSO) was intraplantarly injected into one hindpaw, and the number of flinches was counted for the first 5 min.

Mustard oil test. Mustard oil (1 and 10 µg in 20 µl saline) was injected into the plantar surface of one hindpaw, and the duration of licking and flinching of the injected paw for the first 5 min.

Formalin test. Formalin (5% in 20 µl saline) was injected into the plantar surface of the left hind paw and the duration of licking and flinching was measured in 5 min bins for 45 min after the formalin injection (16).

Primary and secondary mechanical hypersensitivity induced by capsaicin. Capsaicin (5 µg in 10 µl of 2.5% DMSO) was intraplantarly injected into one hindpaw, and primary and secondary mechanical hypersensitivity was assessed by determine the response frequency to a von Frey filament (0.16 g) in the injected site (primary) or surrounding area (secondary) (17).

Motor function testing

A Rota-rod system (IITC Life Science Inc.) was used to assess the motor function. Mice were tested for three trails separated by 10 min intervals. During the tests, the speed of rotation was accelerated from 2 to 20 r.p.m. in 3 min. The falling latency was recorded and averaged (18).

Primary culture of DRG neurons

DRGs were removed aseptically from 4-week old mice and first incubated with collagenase (1.25mg/ml, Roche)/dispase-II (2.4 units/ml, Roche) at 37°C for 90 min, then digested with 0.25% trypsin (Cellgro) for 8 min at 37°C, followed by 0.25% trypsin inhibitor (Sigma). Cells were then mechanically dissociated with a flame polished Pasteur pipette in the presence of 0.05% DNase I (Sigma). DRG cells were plated onto poly-D-lysine and laminin-coated slide chambers (for immunocytochemistry) or glass cover slips (for

electrophysiology) and cultured in a neurobasal defined medium (with 2% B27 supplement, Invitrogen) in the presence of 5 μ M AraC, at 36.5°C, with 5% carbon dioxide.

Single-cell RT-PCR

Single-cell RT-PCR was performed as previously described (19). Briefly, a single cell was aspirated into a patch pipette with a tip diameter of about 25 μ m, gently put into a reaction tube containing reverse transcription reagents, and incubated for 1 hr at 50°C (superscript III, Invitrogen, Carlsbad, CA, USA). The cDNA product was used in separate PCR. The sequences of all the primers used for single-cell PCR are described in table below. The first round of PCR was performed in 50 μ l of PCR buffer containing 0.2 mM dNTPs, 0.2 μ M “outer” primers, 5 μ l RT product and 0.2 μ l platinum Taq DNA polymerase (Invitrogen). The protocol included a 5 min initial denaturation step at 95 °C followed by 40 cycles of 40 s denaturation at 95 °C, 40 s annealing at 55 °C, 40 s elongation at 72 °C. The reaction was completed with 7 min of final elongation. For the second round of amplification, the reaction buffer (20 μ l) contained 0.2 mM dNTPs, 0.2 μ M “inner” primers, 5 μ l of the first round PCR products and 0.1 μ l platinum Taq DNA polymerase. The reaction procedure for these primers was the same as the first round. A negative control was obtained from pipettes that did not harvest any cell contents, but were submerged in the bath solution. The PCR products were displayed on ethidium bromide-stained 1% agarose gels. See **Supplementary Table-1** for the sequences of the primers.

RT-PCR

Total RNAs were isolated from spleen, DRG, brain, and spinal cord tissues of WT and *Tlr3*^{-/-} mice with the RNeasy Mini Kit (QIAGEN) and quantified using A260/A280 absorption. The first-strand cDNAs were synthesized with Oligo(dT)₁₂₋₁₈ primer using SuperScript™ II Reverse Transcriptase (Invitrogen). Mouse PCR primers were designed as follows:

TLR3: sense 5'-CTCTGATGGCTTTGGCTACT-3';
antisense 5'-GATGTTGAACAGGAAGTCGG-3'

GAPDH: sense 5'-GAAGGGTGGAGCCAAAAGG-3';

antisense 5'-AAGGTGGAAGAGTGGGAGTT-3'.

GAPDH were used as an internal control. cDNA samples were amplified for 25-35 cycles by Taq DNA Polymerase (Invitrogen), and PCR products were separated on agarose gel. Gel image were captured in Gel Document System (Bio-Rad).

Real-time quantitative RT-PCR

We collected back hairy skins and cervical DRGs and isolated total RNAs using RNeasy Plus Mini kit (Qiagen, Valencia, CA). One microgram of RNA was reverse transcribed for each sample using Omniscript reverse transcriptase according to the protocol of the manufacturer (Qiagen). Sequences for the forward and reverse primers for TLR2, TLR3, TLR4, TLR7, TLR9, Tryptase, Chymases, CD117 and NGF are described in the **Supplementary Table 2**. Triplicate qPCR analyses were performed using the SYBR Green master mix (KAPA) and Opticon real-time PCR Detection System (Bio-Rad, Hercules, CA) as described previously (20).

Extraction of total RNAs for electrophysiology

Total RNAs were extracted from mouse brains using an RNeasy Plus Mini Kit (Qiagen). gDNA eliminator columns were used to remove potential genomic DNA contamination according to the protocol developed by Qiagen. The quality of the total RNAs were tested using NanoDrop (Thermo Scientific) before use.

Patch-clamp recordings in dissociated DRG neurons

As we previously described (7), whole-cell voltage- and current-clamp recordings were performed at room temperature to measure currents and action potentials (APs), respectively, with Axopatch-200B amplifier (Axon Instruments, Union City, USA). The patch pipettes were pulled from borosilicate capillaries (Chase Scientific Glass Inc., Rockwood, CA, USA). When filled with the pipette solution, the resistance of the pipettes was 4 ~ 5 M Ω . The recording chamber (volume 300 μ l) was continuously superfused (2 ~ 3 ml/min). Series resistance was compensated for (> 80%), and leak subtraction was performed. Data were low-pass-filtered at 2 KHz, sampled at 10 KHz. The pClamp8 (Axon Instruments) software was used during experiments and analysis.

The pipette solution for voltage-clamp experiments was composed of (in mM): 126 K-gluconate, 10 NaCl, 1 MgCl₂, 10 EGTA, 2 NaATP, and 0.1 MgGTP, adjusted to pH 7.4 with KOH, osmolarity 295 - 300 mOsm. Extracellular solution for voltage-clamp experiments contained (in mM): 140 NaCl, 5 KCl, 2 CaCl₂, 1 MgCl₂, 10 HEPES, 10 glucose, adjusted to pH 7.4 with NaOH and osmolarity 300-310 mOsm. Voltage-clamp experiments were performed at a holding potential of -60 mV. The pipette solution for current-clamp experiments was composed of (in mM): 145 K-gluconate, 2 MgCl₂, 1 CaCl₂, 10 EGTA, 5 HEPES, 5 K₂ATP, adjusted to pH 7.3–7.4 with KOH, osmolarity 300 mOsm. Extracellular solution for current-clamp experiments contained (in mM): 140 NaCl, 5 KCl, 2 CaCl₂, 1 MgCl₂, 10 HEPES, and 10 glucose, adjusted to pH 7.4 with NaOH and osmolarity 300-310 mOsm.

Spinal cord slice preparation and patch clamp recordings

As we previously reported (21), a portion of the lumbar spinal cord (L4-L5) was removed from mice (4-6 week old) under urethane anesthesia (1.5 - 2.0 g/kg, i.p.) and kept in pre-oxygenated ice-cold Krebs solution. Transverse slices (400-600 μ m) were cut on a vibrating microslicer. The slices were perfused with Krebs's solution (8-10 ml/min) that was saturated with 95% O₂ and 5% CO₂ at 36 \pm 1 $^{\circ}$ C for at least 1-3 h prior to experiment. The Krebs's solution contains (in mM): NaCl 117, KCl 3.6, CaCl₂ 2.5, MgCl₂ 1.2, NaH₂PO₄ 1.2, NaHCO₃ 25, and glucose 11. The whole cell patch-clamp recordings were made from lamina IIo neurons in voltage clamp mode. Patch pipettes were fabricated from thin-walled, borosilicate, glass-capillary tubing (1.5 mm o.d., World Precision Instruments). After establishing the whole-cell configuration, neurons were held at the potential of -70 mV to record sEPSCs. The resistance of a typical patch pipette is 5-10 M Ω . The internal solution contains (in mM): potassium gluconate 135, KCl 5, CaCl₂ 0.5, MgCl₂ 2, EGTA 5, HEPES 5, ATP-Mg 5. Membrane currents were amplified with an Axopatch 200B amplifier (Axon Instruments) in voltage-clamp mode. Signals were filtered at 2 kHz and digitized at 5 kHz. Data were stored with a personal computer using pCLAMP 10 software and analyzed with Mini Analysis (Synaptosoft Inc.).

Spinal cord LTP recordings in anesthetized mice

Mice were anesthetized with urethane (1.5 g/kg, IP). The trachea was cannulated to allow mechanical ventilation, if necessary. PBS (0.5-1 ml, i.p.) was injected prior to surgery and every 2 h after surgery to maintain electrolyte balance. A laminectomy was performed at vertebrae T13-L1 to expose the lumbar enlargement, and the left sciatic nerve was exposed for bipolar electrical stimulation. The vertebral column was firmly suspended by rostral and caudal clamps on the stereotaxic frame. The exposed spinal cord and the sciatic nerve were covered with paraffin oil. Colorectal temperature was kept constant at 37-38°C by a feedback-controlled heating blanket. Following electrical stimulation of the sciatic nerve, the field potentials were recorded in the ipsilateral L4-5 spinal cord segments with glass microelectrodes, 100-300 µm from the surface of the cord. *In vivo* LTP was recorded as we previously reported (22). After recording stable responses following test stimuli (2x C-fiber threshold, 0.5 ms, 1 min interval, every 5 min) for > 40 min, conditioning tetanic stimulation (5 times of C-fiber threshold, 100 Hz, 1 s, 4 trains, 10 s interval) was delivered to the sciatic nerve for inducing LTP of C-fiber-evoked field potentials.

In situ hybridization

Mice were terminally anesthetized with isoflurane and transcardially perfused with PBS and 4% paraformaldehyde. DRGs were collected and post-fixed overnight. DRG tissues were sectioned in a cryostat at a thickness of 12 µm and mounted on Superfrost plus slides. Two separate TLR3 riboprobes (0.34 and 0.76kb) and a riboprobe for pan-neuronal marker SCG10 were generated by PCR. The reverse primer contains T7 RNA polymerase binding sequence (TGTAATACGACTCACTATAGGGCG) for the generation of the antisense riboprobe. DNA sequences were transcribed *in vitro* with T7 RNA polymerase (Promega) in the presence of digoxigenin-labeling mix. *In situ* hybridization was performed as we previously described (23, 24). Briefly, sections were hybridized with TLR3 riboprobe (1 µg/ml) or SCG10 riboprobe (1 µg/ml) overnight at 65°C. After washing, sections were blocked with 20% serum for 1 h at room temperature followed by incubation with alkaline phosphatase-conjugated anti-digoxigenin antibody (1:2000; Roche Diagnostics) overnight at 4°C. Sections were then incubated with a mixture of nitro-blue tetrazolium (NBT) and 5-bromo-4-chloro-3-indolyl-phosphate (BCIP) in alkaline phosphatase buffer for 24-48 h for

color development. *In situ* hybridization images were captured with a Nikon microscope under bright-field.

Immunohistochemistry

Mice were terminally anesthetized with isoflurane and perfused through the ascending aorta with saline followed by 4% paraformaldehyde. We collected DRGs, dorsal roots, sciatic nerves, skins, and spinal cords and postfixed these tissues in the same fixative overnight. The DRG, dorsal root, and sciatic nerve sections were cut at the thickness of 14- μ m and the spinal cord sections (free floating) were cut at the thickness of 30- μ m in a cryostat. The tissue sections were blocked with 2% goat serum, and incubated over night at 4°C with the primary antibodies. The sections were then incubated for 1 h at room temperature with Cy3- or FITC- conjugated secondary antibodies. For double immunofluorescence, sections were incubated with a mixture of polyclonal and monoclonal primary antibodies followed by a mixture of FITC- and CY3-conjugated secondary antibodies (25). Immunostained tissue sections were examined under a Nikon fluorescence microscope, and images were captured with a high resolution CCD Spot camera (Diagnostic Instruments Inc.) and analyzed with NIH Image software or Adobe PhotoShop.

To determine pruritogen-induced Fos expression in the spinal cord, 2 h after intradermal injection of pruritogens (compound 48/80 or chloroquine), the mice were terminally anesthetized with isoflurane and perfused through the ascending aorta with saline followed by 4% paraformaldehyde. The cervical spinal cords were collected for c-Fos immunofluorescence.

We used the following primary antibodies for immunofluorescence: rabbit anti-TLR3 antibody (1:1000, Santa Cruz), guinea pig anti-TRPV1 antibody (1:1000, Neuromics), rabbit anti-GRP antibody (1:1000, Immunostar), guinea pig anti-Substance P antibody (1:1000, Neuromics), rabbit anti-Fos antibody (1:500, Santa Cruz), mouse anti-NF200 (1:2000, Sigma), mouse anti-NeuN antibody (1:2000, Millipore), rabbit anti-CGRP antibody (1: 2000, Neuromics), rabbit anti-PKC γ antibody (1:2000, Santa Cruz), rabbit anti-PGP9.5 antibody (1:1000, Biogenesis).

To enhance the signal of GRP immunostaining, TSA (Tyramide Signal Amplification) kit (Perkin Elmer, MA) was used for some tissue sections. In brief, after the

primary antibody incubation, the sections were incubated with a biotinylated-secondary antibody (1:400, 1 h at room temperature), followed by avidin-streptin incubation (1:100, 1 h at room temperature), and finally by tyramide incubation (1:50, 5 min at room temperature).

We also performed immunostaining on cultured DRG neurons. DRG cultures were prepared as above described and were grown in slide chambers for 24 hours and fixed with 4% paraformaldehyde for 30 min. Cells were then incubated with a mixture of primary antibodies of TLR3 (rabbit, Santa Cruz, 1:500), NF-200 (Mouse, sigma, 1:500) and TRPV1 (guinea pig, 1:500, Chemicon), overnight, following by a mixture of Cy3- and FITC-conjugated secondary antibodies. Images were visualized and analysis using fluorescence microscope (Nikon) or confocal microscope (LSM 510 META, Carl Zeiss MicroImaging Inc.).

Calcium imaging from cultured DRG neurons

DRGs from all spinal levels of 4-week old mice were collected in cold DH10 (90% DMEM/F-12, 10% FBS, 100 U/ml penicillin, and 100 µg/ml Streptomycin, Gibco) and treated with enzyme solution (5 mg/ml Dispase, 1 mg/ml Collagenase Type I in HPBS without Ca⁺⁺ and Mg⁺⁺, Gibco) at 37°C. Following trituration and centrifugation, cells were resuspended in DH10, plated on glass cover slips coated with poly-D-lysine (0.5 mg/ml, Stoughton, MA) and laminin (10 µg/ml, Invitrogen), cultured in an incubator (95% O₂ and 5% CO₂) at 37°C and used within 24 hours. Neurons were loaded with Fura 2-acetomethoxy ester (Molecular Probes) for 30 min in the dark at room temperature. After washing, cells were imaged at 340 and 380 nm excitation to detect intracellular free calcium. To compare the response to histamine, chloroquine, and capsaicin between WT and Tlr3-deficient DRG neurons, calcium imaging assays were performed with an experimenter blind to genotype (n=3 per genotype), and the percentages of DRG neurons showing calcium responses were determined as we previously described (26).

Western blotting

Mice were terminally anesthetized with isoflurane and transcardially perfused with PBS, and the DRGs were rapidly removed and homogenized in a lysis buffer containing a

cocktail of protease inhibitors and phosphatase inhibitors. The protein concentrations were determined by BCA Protein Assay (Pierce), and 30 µg of proteins were loaded for each lane and separated on SDS-PAGE gel (4-15%, Bio-Rad). After the transfer, the blots were incubated overnight at 4°C with polyclonal antibody against TLR3 (rabbit, 1:500, Imgenex). For loading control, the blots were probed with GAPDH antibody (rabbit, 1:10000, Sigma).

Histology

Mice were terminally anesthetized with isoflurane and the back hairy skins and hindpaw skins were collected from 4 pairs of wild-type and *Tlr3* knockout to perform histological examination. Tissues were postfixed in 4% paraformaldehyde overnight and skin sections were cut (14 µm) in a cryostat. The sections were stained with toluidine blue (TB) for mast cells and also processed for hematoxylin & eosin (H&E) staining for hair follicle examination. Hair follicles during deferent growth cycles were identified as previously reported (27, 28). The stained sections were then dried, cleared, and covered for observation and photomicrography. The number of mast cells and hair follicles at different cycle stages was quantified by individuals that are blinded for the genotype using 10 sections per mouse and 4 mice per group.

Histamine measurement

Mice were terminally anesthetized with isoflurane and the back hairy skins were collected from 4 pairs of WT and *Tlr3*^{-/-} mice to measure the histamine content. Histamine was quantified using a histamine Enzyme Immunoassay kit (Oxford Biomedical Research) according to the manufacture's manual. Histamine was also measured in the back skins after AEW treatment in WT and *Tlr3*^{-/-} mice. We also measured histamine release in skin organ cultures after treatment of compound 48/80 (100 µg/ml, 30 min).

Quantification

To determine if there are changes in neurochemical markers and loss of neurons in the DRGs of *Tlr3* deficient mice, L4/L5 lumbar DRGs were dissected from 4 pairs of mutant and control mice, and every eighth section (12-µm thickness) was used for immunostaining

(CGRP, NF-200, and P2X3). Around 14-17 sections from each DRG were chosen for the quantification of each immunostaining (**Supplementary Table-3**). Only those neurons showing nuclei and distinct staining above the background were counted. This semi-quantification was based on the fact that the sizes of DRG neurons in *Tlr3*-KO mice did not change. We did not intend to determine the actual number of neurons. Rather, we used this method to compare the difference (percentage of positive neurons in DRG) between WT and KO mice.

Statistics

All the data are expressed as mean \pm SEM. Most data were analyzed with two-tailed Student's *t*-test (mainly for two groups of WT and KO mice) to determine statistically significant differences. One-way ANOVA followed by post-hoc Bonferroni test was used for multiple comparisons. Two-Way repeated measured ANOVA was also used to analyze the data with multiple time points (e.g. data of LTP and time course of itch behavior). The criterion for statistical significance was $P < 0.05$.

Study approval

All animal procedures performed in this study were reviewed and approved by the Harvard Medical Area Standing Committee on Animals. The experiments were conducted in accordance with the NIH guidelines for care and use of animals and the recommendations of International Association for the Study of Pain.

Supplementary references

1. Alexopoulou L, Holt AC, Medzhitov R, Flavell RA. Recognition of double-stranded RNA and activation of NF-kappaB by Toll-like receptor 3. *Nature*. 2001;413(6857):732-738.
2. Obata K, et al. Toll-like receptor 3 contributes to spinal glial activation and tactile allodynia after nerve injury. *J Neurochem*. 2008;105(6):2249-2259.
3. Kawasaki Y, et al. Distinct roles of matrix metalloproteases in the early- and late-phase development of neuropathic pain. *Nat Med*. 2008;14(3):331-336.
4. Xu ZZ, et al. Resolvins RvE1 and RvD1 attenuate inflammatory pain via central and peripheral actions. *Nat Med*. 2010;16(5):592-7, 1p.
5. Sun YG, Chen ZF. A gastrin-releasing peptide receptor mediates the itch sensation in the spinal cord. *Nature*. 2007;448(7154):700-703.
6. Sun YG, Zhao ZQ, Meng XL, Yin J, Liu XY, Chen ZF. Cellular basis of itch sensation. *Science*. 2009;325(5947):1531-1534.
7. Liu T, Xu ZZ, Park CK, Berta T, Ji RR. Toll-like receptor 7 mediates pruritus. *Nat Neurosci*. 2010;13(12):1460-1462.
8. Shimada SG, LaMotte RH. Behavioral differentiation between itch and pain in mouse. *Pain*. 2008;139(3):681-687.
9. Klein AH, Iodi CM, Carstens E. Facial injection of pruritogens or algogens elicit distinct behavior responses in rats and excite overlapping populations of trigeminal neurons. *J Neurophysiol*. 2011;106(3):1078-1088.
10. Miyamoto T, Nojima H, Shinkado T, Nakahashi T, Kuraishi Y. Itch-associated response induced by experimental dry skin in mice. *Jpn J Pharmacol*. 2002;88(3):285-292.
11. Akiyama T, Carstens MI, Carstens E. Enhanced responses of lumbar superficial dorsal horn neurons to intradermal PAR-2 agonist but not histamine in a mouse hindpaw dry skin itch model. *J Neurophysiol*. 2011;105(6):2811-2817.
12. Dixon WJ. Efficient analysis of experimental observations. *Annu Rev Pharmacol Toxicol*. 1980;20:441-462.
13. RANDALL LO, SELITTO JJ. A method for measurement of analgesic activity on inflamed tissue. *Arch Int Pharmacodyn Ther*. 1957;111(4):409-419.

14. Hargreaves K, Dubner R, Brown F, Flores C, Joris J. A new and sensitive method for measuring thermal nociception in cutaneous hyperalgesia. *Pain*. 1988;32(1):77-88.
15. Ramabadran K, Bansinath M, Turndorf H, Puig MM. Tail immersion test for the evaluation of a nociceptive reaction in mice. Methodological considerations. *J Pharmacol Methods*. 1989;21(1):21-31.
16. Zhang L, Berta T, Xu ZZ, Liu T, Park JY, Ji RR. TNF-alpha contributes to spinal cord synaptic plasticity and inflammatory pain: distinct role of TNF receptor subtypes 1 and 2. *Pain*. 2011;152(2):419-427.
17. Schwartz ES, Lee I, Chung K, Chung JM. Oxidative stress in the spinal cord is an important contributor in capsaicin-induced mechanical secondary hyperalgesia in mice. *Pain*. 2008;138(3):514-524.
18. Malmberg AB, Gilbert H, McCabe RT, Basbaum AI. Powerful antinociceptive effects of the cone snail venom-derived subtype-selective NMDA receptor antagonists conantokins G and T. *Pain*. 2003;101(1-2):109-116.
19. Park CK, et al. Substance P sensitizes P2X3 in nociceptive trigeminal neurons. *J Dent Res*. 2010;89(10):1154-1159.
20. Berta T, Poirot O, Pertin M, Ji RR, Kellenberger S, Decosterd I. Transcriptional and functional profiles of voltage-gated Na(+) channels in injured and non-injured DRG neurons in the SNI model of neuropathic pain. *Mol Cell Neurosci*. 2008;37(2):196-208.
21. Kawasaki Y, Zhang L, Cheng JK, Ji RR. Cytokine mechanisms of central sensitization: distinct and overlapping role of interleukin-1beta, interleukin-6, and tumor necrosis factor-alpha in regulating synaptic and neuronal activity in the superficial spinal cord. *J Neurosci*. 2008;28(20):5189-5194.
22. Park CK, Lu N, Xu ZZ, Liu T, Serhan CN, Ji RR. Resolving TRPV1- and TNF-alpha-mediated spinal cord synaptic plasticity and inflammatory pain with neuroprotectin D1. *J Neurosci*. 2011;31(42):15072-15085.
23. Chen CL, et al. Runx1 determines nociceptive sensory neuron phenotype and is required for thermal and neuropathic pain. *Neuron*. 2006;49(3):365-377.
24. Gao YJ, et al. JNK-induced MCP-1 production in spinal cord astrocytes contributes to central sensitization and neuropathic pain. *J Neurosci*. 2009;29(13):4096-4108.
25. Jin SX, Zhuang ZY, Woolf CJ, Ji RR. p38 mitogen-activated protein kinase is activated after a spinal nerve ligation in spinal cord microglia and dorsal root ganglion neurons and contributes to the generation of neuropathic pain. *J Neurosci*. 2003;23(10):4017-4022.

26. Liu Q, et al. Sensory neuron-specific GPCR Mrgprs are itch receptors mediating chloroquine-induced pruritus. *Cell*. 2009;139(7):1353-1365.
27. Paus R, Cotsarelis G. The biology of hair follicles. *N Engl J Med*. 1999;341(7):491-497.
28. Lyubimova A, et al. Neural Wiskott-Aldrich syndrome protein modulates Wnt signaling and is required for hair follicle cycling in mice. *J Clin Invest*. 2010;120(2):446-456.

Supplementary Table-1. Sequences of outer and inner primers for single-cell PCR.

Target gene (Product length) ^a	Outer primers	Inner primers	Genbank No.
TRPV1 (273 bp, 203 bp)	TGATCATCTTCACCACGGCTG CCTTGGGATGGCTGAAGTACA	AAGGCTTGCCCCCTATAA CACCAGCATGAACAGTGACTGT	NM_001001445.1
GRP (258 bp, 201 bp)	CCAAGGAGCAAACAAAACCC GCAAATTGGAGCCCTGAATCT	AGACTGCCTTCTGCAAACGTC AAGCCTAGCTGGAAAAAGCG	NM_175012.2
GAPDH (367 bp, 313 bp)	AGCCTCGTCCCGTAGACAAA TTTTGGCTCCACCCCTCA	TGAAGGTCGGTGTGAACGAATT GCTTCTCCATGGTGGTGAAGA	XM_001473623.1
TLR3 (477 bp, 269 bp)	CCAGTTCCTTGCATTGGTCC GCCCCAAAACATCCTTCTCAA	CAGCCTTCAAAGACTGATGCTC GATTCATCTAAGCCGTTGGAC	NM_126166.4
TLR7 (421 bp, 359 bp)	CAGTGAACCTGGCCGTTGAGA TGCGGCATACCCTCAAAA	TTCTCCAACAACCGGCTTGAT TCAGGAGGCAAGGAATTCAGG	NM_133211.3

^a (n, n) indicates product size obtained from outer and inner primers, respectively.

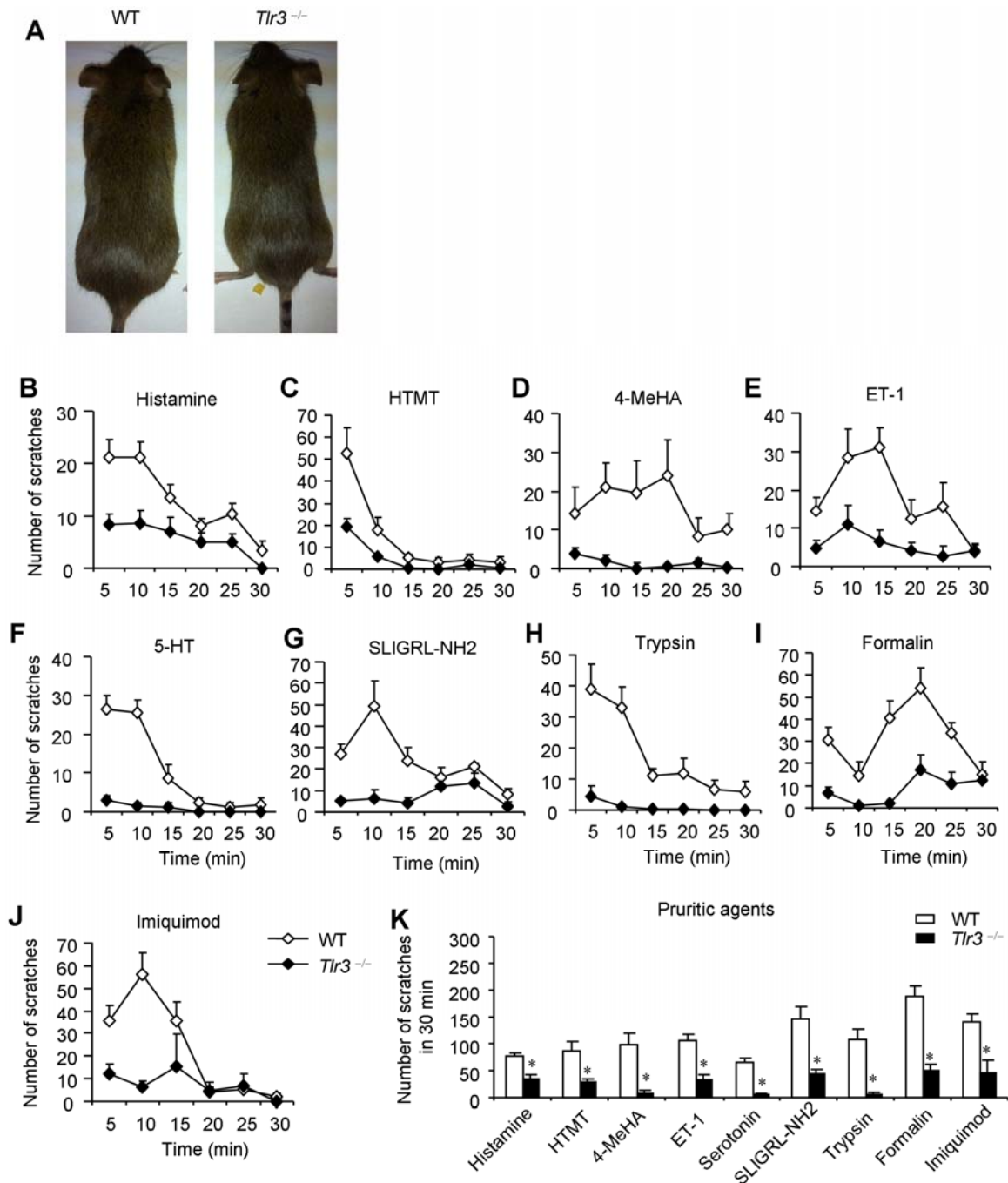
Supplementary Table-2. Sequences of primers for quantitative real-time PCR

Target gene	Forward primers	Reverse primers	Genbank No.
GAPDH	TCC ATG ACA ACT TTG GCA TTG	CAG TCT TCT GGG TGG CAG TGA	XM_001473623
TLR2	ACA ACT TAC CGA AAC CTC AGA	ACC CCA GAA GCA TCA CAT G	NM_011905
TLR3	GCG TTG CGA AGT GAA GAA CT	TTC AAG AGG AGG GCG AAT AA	NM_126166
TLR4	TTC AGA ACT TCA GTG GCT GG	TGT TAG TCC AGA GAA ACT TCC TG	NM_021297
TLR 7	TTT GTC TCT TCC GTG TCC AC	GAT GTC CTT GGC TCC CTTT C	NM_133211
TLR 9	AAC CGC CAC TTC TAT AAC CAG	GTA AGA CAG AGC AAG GCA GG	NM_031178
TRPV1	ATG TTC GTC TAC CTC GTG TTC TTG	AGG CAG TGA GTT ATT CTT CCC ATC C	NM_001001445
TAC1 (SP)	AGG CTC TTT ATG GAC ATG GC	TCT TTC GTA GTT CTG CAT CGC	NM_009311
TNF alpha	CCC CAA AGG GAT GAG AAG TT	CAC TTG GTG GTT TGC TAC GA	NM_013693
NGF	CCC AAT AAA GGT TTT GCC AAG G	TTG CTA TCT GTG TAC GGT TCT G	NM_013609
TPSAB1	ATT TCT GAC TAT GTC CAC CCT G	AAT GGG AAC TTG CAC CTC C	NM_031187
CMA1	CAC TTC TGA GAA CTA CCT GTC G	TGT TTT GTT ATG GGC TCC TAG G	NM_010780
KIT (CD117)	TGT GGC TAA AGA TGA ACC CTC	ACA CTC CAG AAT CGT CAA CTC	NM_021099

Supplementary Table-3. Example of quantification for immunostaining (TRPV1, P2X3, NF-200, and CGRP) in every 8th section from a WT mouse DRG and a *Tlr3*-KO mouse DRG.

WT animal #3 n=16 sections							KO animal #4 n=17 sections						
DRG							DRG						
SECTION	SCG10	TRPV1	P2X3	NF200	CGRP	CGRP(ISH)	SECTION	SCG10	TRPV1	P2X3	NF200	CGRP	CGRP(ISH)
1	34	12	3	3	8	6	1	25	6	11	3	7	13
2	37	14	5	3	12	7	2	37	10	10	5	11	11
3	61	13	7	6	18	7	3	42	13	11	6	15	16
4	81	22	11	7	21	18	4	57	17	7	11	23	19
5	125	28	16	15	41	13	5	78	15	22	10	34	19
6	119	38	27	13	31	28	6	117	23	32	12	36	30
7	140	41	34	12	39	35	7	131	27	27	17	43	39
8	140	47	39	9	48	61	8	116	26	43	24	43	32
9	172	54	45	18	47	57	9	153	36	36	19	42	52
10	163	36	43	13	51	47	10	173	41	46	17	46	53
11	156	37	37	12	38	35	11	158	51	37	10	47	46
12	120	24	41	23	29	38	12	140	49	51	11	45	46
13	124	22	26	17	30	21	13	140	29	42	21	42	29
14	100	21	31	14	18	21	14	120	30	36	16	34	19
15	87	22	25	10	13	19	15	84	16	32	10	35	19
16	41	14	11	1	2	4	16	76	19	14	5	13	13
							17	19	5	3	4	4	6
Sum	11900	3115	2807	1232	3122	2919	Sum	11662	2891	3220	1407	3640	3234
%		26.18	23.59	10.35	26.24	24.53	%		24.79	27.61	12.06	31.21	27.73

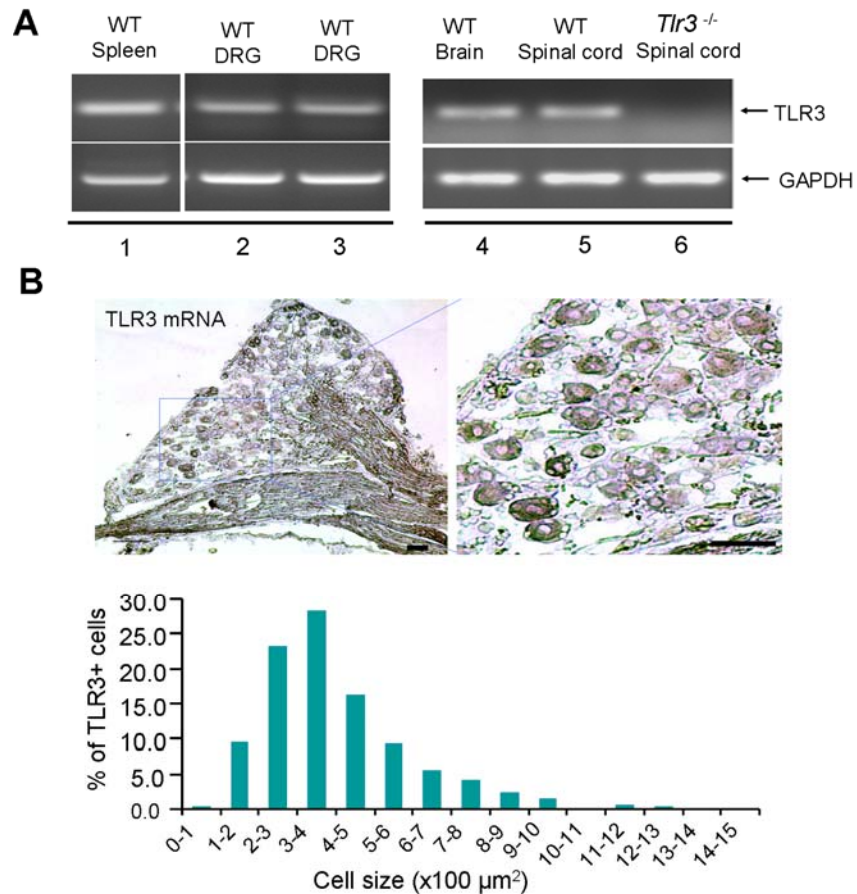
The total number of neurons was obtained by SCG10 mRNA staining using in situ hybridization in adjacent DRG sections. The % of positive neurons of each immunostaining was calculated by the number of immuno-positive cells / number of SCG10-positive cells in a given DRG. The data show no difference between WT and KO mice for all the neurochemical markers we examined in the DRGs.



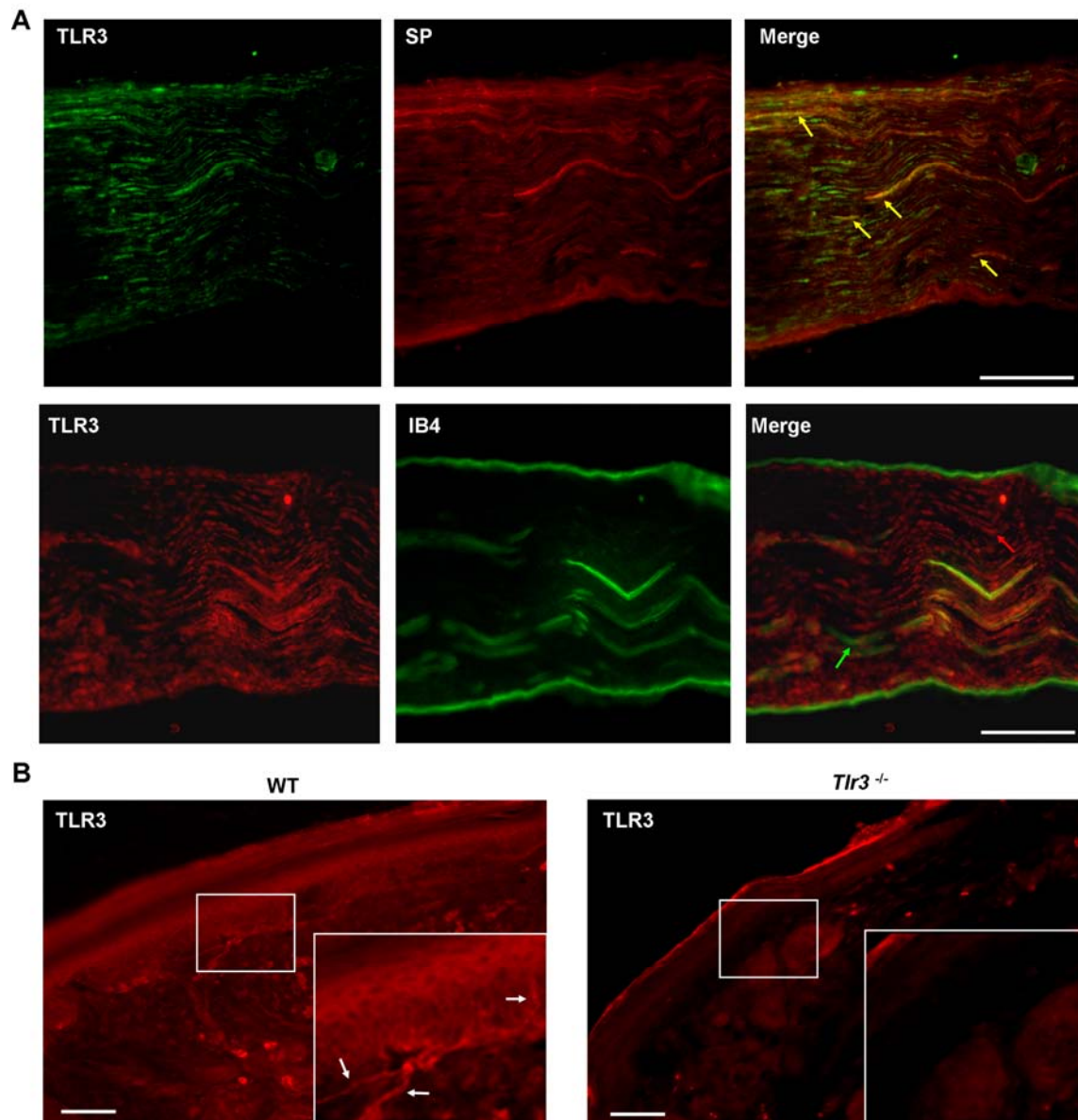
Supplementary Figure 1. *Tlr3*^{-/-} mice display normal anatomy but impaired scratching behaviors induced by both histamine-dependent and independent pruritic agents.

(A) Photographs of WT and *Tlr3*^{-/-} mice. Note there are no changes in gross anatomy of the KO mice. (B-J) Time course of scratching responses in 30 min in *Tlr3*^{-/-} mice and WT mice,

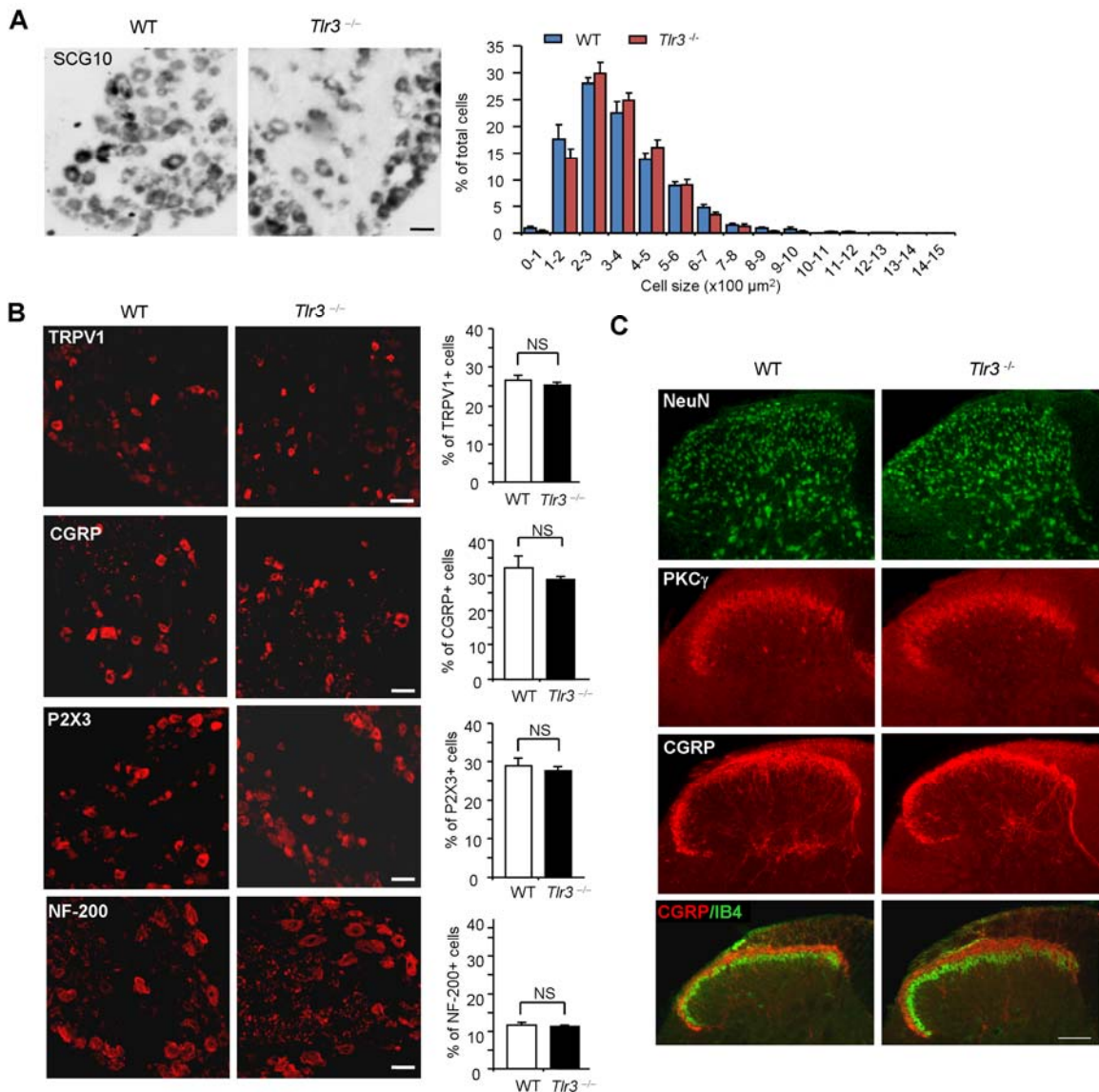
following intradermal injection of 50 μ l of pruritic agents, including histamine (B; 500 μ g), HTMT (C; H1 receptor agonist; 100 μ g), 4-MeHA (D; histamine H4 receptor agonist; 500 μ g), endothelin-1 (E; ET-1; 25 ng), serotonin (F; 5-HT; 20 μ g), SLIGRL-NH2 (G; PAR2 agonist; 100 μ g), trypsin (H; 300 μ g), formalin (I; 0.6%) and imiquimod (J; TLR7 agonist; 100 μ g) in WT and *Tlr3*^{-/-} mice. $P < 0.05$ in all the panels, Two-way repeated measures ANOVA. (K) Histogram shows the summary of scratches in 30 min following intradermal injection of pruritic agents. * $P < 0.05$, Student's t-test, n=5-9 mice.



Supplementary Figure 2. TLR3 is expressed in DRG neurons of adult mice. (A) RT-PCR analysis shows TLR3 mRNA expression in spleen, DRG, brain and spinal cord tissues. The lanes in the left panel ran on the same gel but were noncontiguous. Note that TLR3 expression was absent in *Tlr3*^{-/-} mice. (B) *In situ* hybridization showing TLR3 mRNA expression in DRG neurons. Scale, 50 μm. Lower lane, cell size distribution analysis of TLR3 mRNA-expressing neurons. Note that TLR3 is mainly expressed in small-sized and some medium-sized DRG neurons.

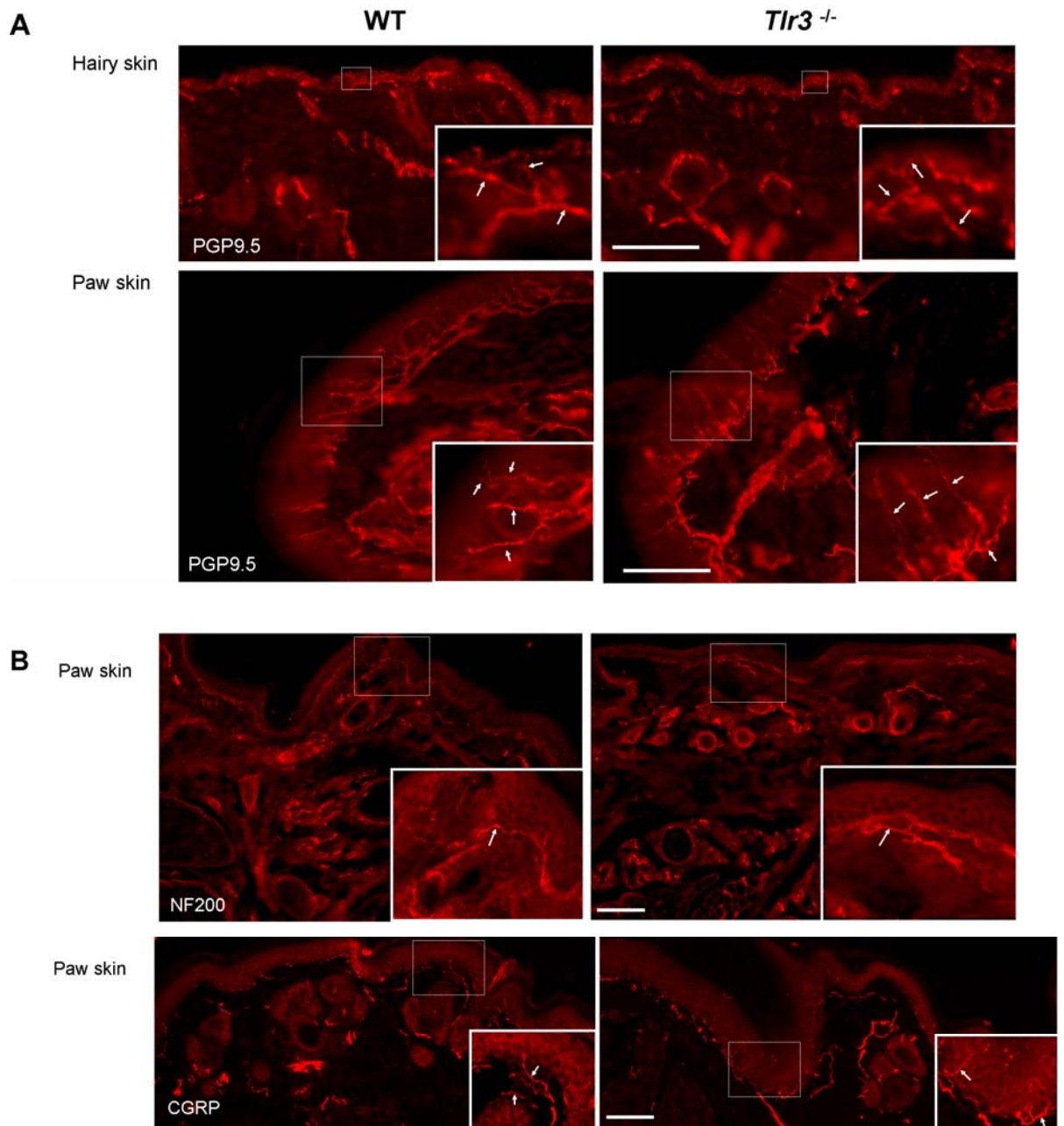


Supplementary Figure 3. TLR3 is expressed in the sciatic nerve axons and skin nerve endings in mice. (A) Double immunohistochemistry of TLR3/substance P (SP) and TLR3/IB4 in the sciatic nerve. Note colocalization of TLR3 and SP in the axons. Yellow arrows indicate double-labeled axons, and green and red arrows show singly-labeled axons. Scales, 50 μ m. (B) Left panel: immunohistochemistry showing TLR3 expression in the skin nerve terminals. Arrows indicate the TLR3-positive nerve endings. Note that TLR3 is also expressed in keratinocytes in the epidermis. Right panel: TLR3 staining in skin section of *Tlr3*^{-/-} mice. Note that TLR3+ signaling in nerve terminals and keratinocytes is absent in the KO mice. The remaining staining in KO mice could be non-specific. The small box is enlarged in the large box. Scales, 50 μ m.

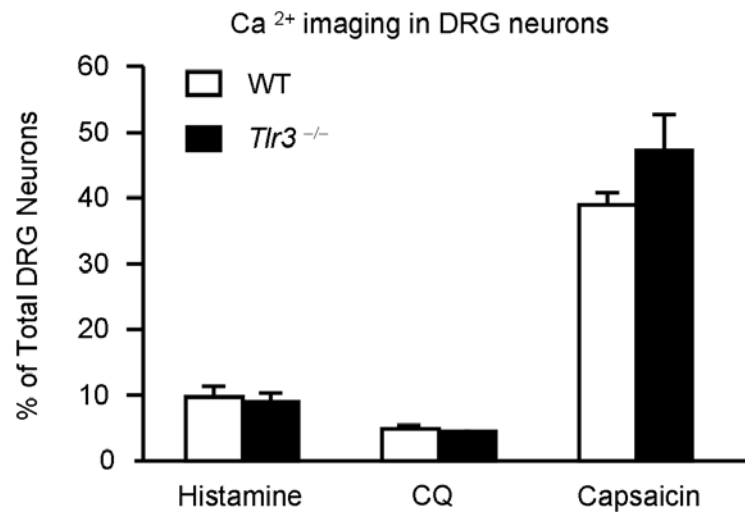


Supplemental Figure 4. Normal expression of neuronal markers in the DRGs and spinal cords of *Tlr3*^{-/-} mice. (A) *In situ* hybridization of pan-neuronal marker SCG-10 reveals no obvious neuronal loss in the DRG of *Tlr3*^{-/-} mice. Right panel shows similar cell-size distribution of SCG-10 mRNA-positive neurons in WT and *Tlr3*^{-/-} mice. (B) Immunohistochemistry shows no change in the expression of TRPV1, CGRP, P2X3 and NF200 in the DRGs of *Tlr3*^{-/-} mice. Right graphs show the percentile of immunoreactive neurons in DRGs of WT and KO mice ($P > 0.05$, Student's *t* test, $n = 4$ mice). Also see Supplemental Table-3 for an example of quantification. (C) *Tlr3*^{-/-} mice show normal distribution patterns in the

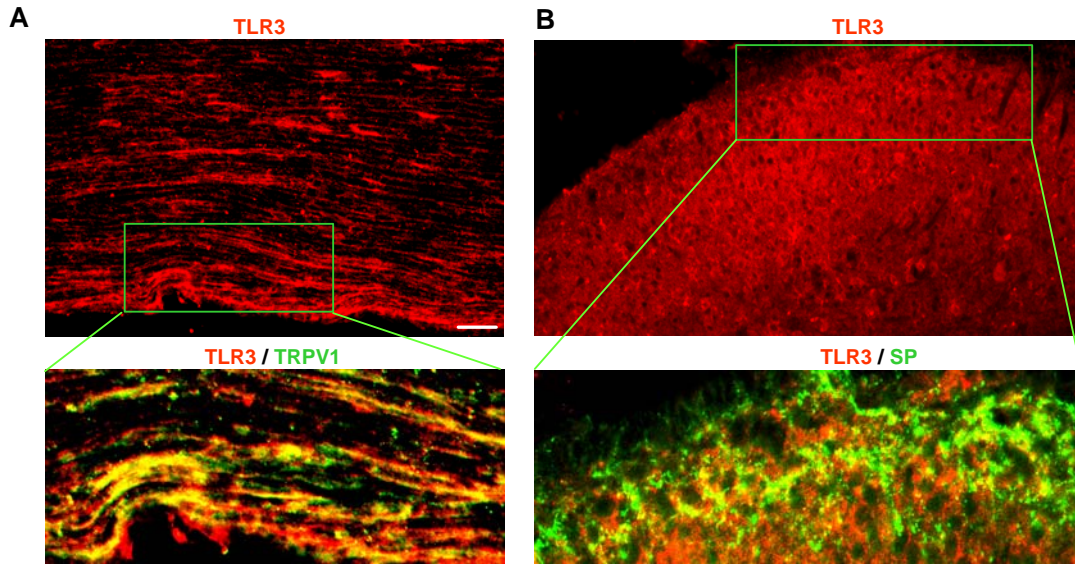
spinal cord dorsal horn of the neurochemical markers NeuN and PKC γ and normal innervations of the primary afferents labeled with CGRP and IB4. Notice that CGRP+ peptidergic (red) and IB4+ non-peptidergic (green) primary afferents are well separated in the superficial dorsal horn of *Tlr3*^{-/-} mice. Scales, 100 μ m.



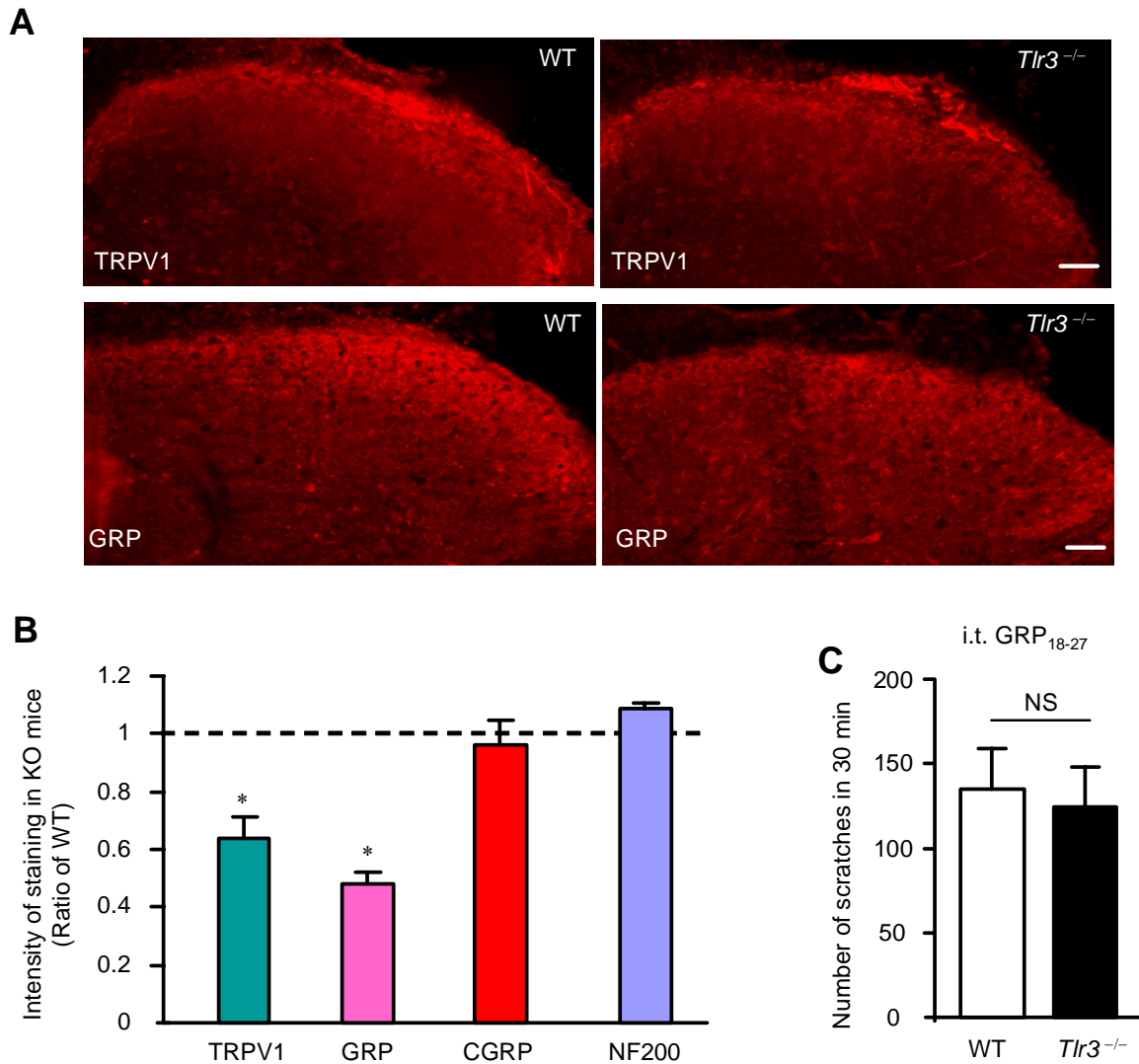
Supplementary Figure 5. (A) Immunostaining of PGP9.5 (a pan neuronal marker) in the hairy skins (upper panel) and paw glabrous skins (lower panel) of WT and *Tlr3*^{-/-} mice. Scales, 100 μ m. **(B)** Immunostaining of NF200 (a myelinated A-fiber marker, upper panel) and CGRP (a marker for peptidergic fibers, lower panel) in the paw skins of WT and *Tlr3*^{-/-} mice. Scales, 50 μ m. Note that *Tlr3*^{-/-} mice display normal nerve innervations in the skins.



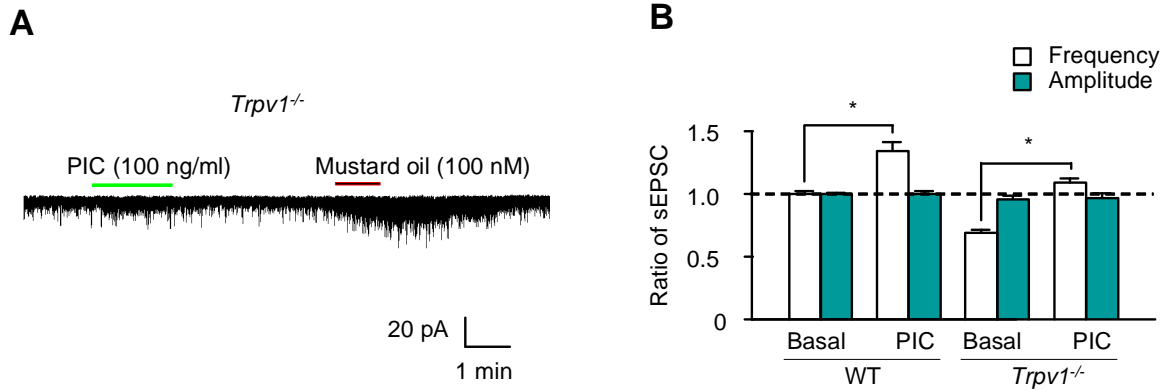
Supplementary Figure 6. Ca²⁺ imaging analysis shows that DRG neurons of WT and *Tlr3*^{-/-} mice have similar Ca²⁺ responses to capsaicin, histamine, and chloroquine (CQ). n=3 mice per genotype.



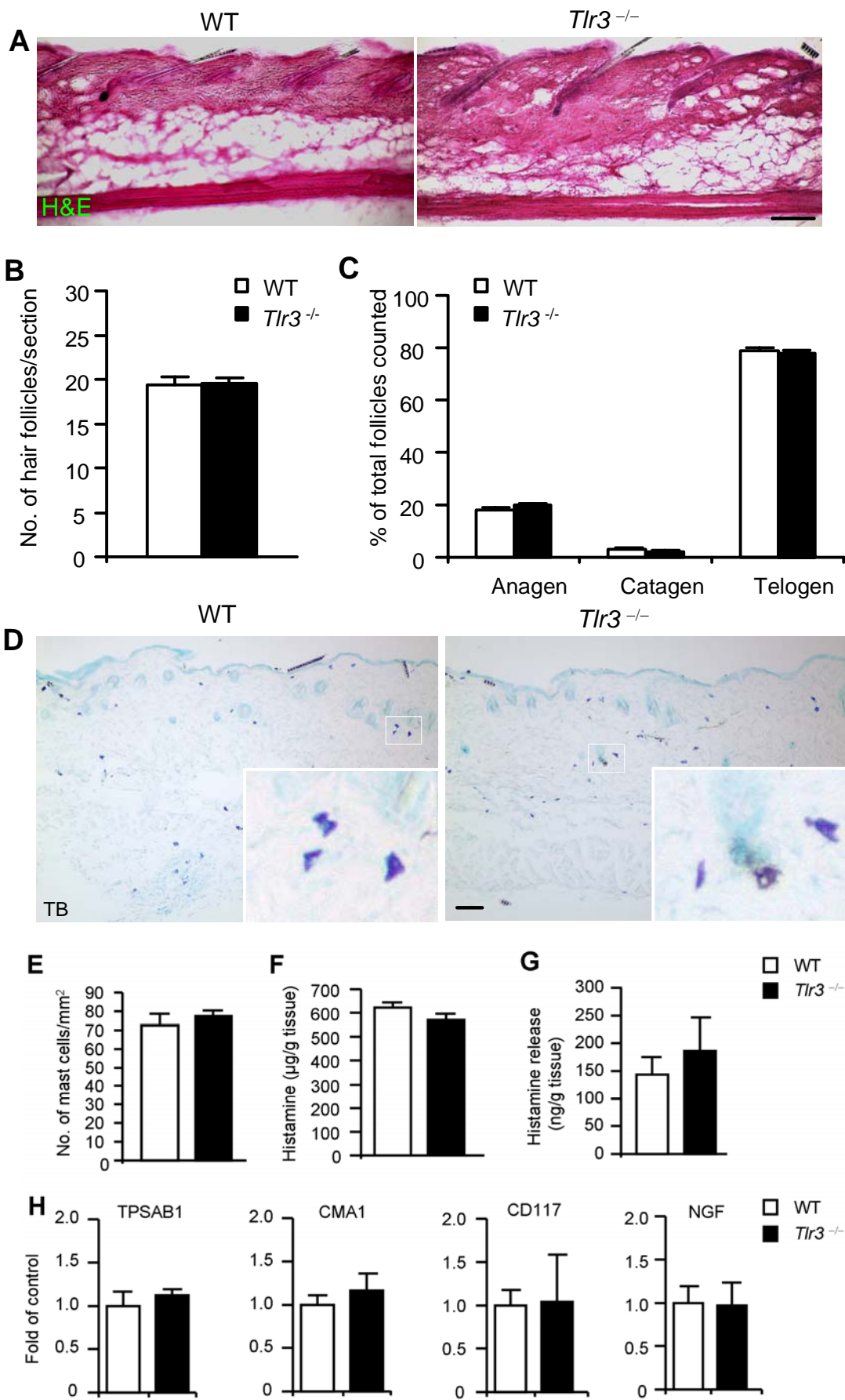
Supplementary Figure 7. TLR3 expression in the central axons and axonal terminals of DRG neurons. (A) Single and double immunohistochemistry in the dorsal roots showing TLR3 expression in the axons (upper panel) and its colocalization with TRPV1 (lower panel). (B) Single and double immunohistochemistry showing TLR3 expression in the spinal cord dorsal horn axonal terminals (upper panel) and its colocalization with substance P (SP). Lower panels are enlargements of small boxes in upper panels. Scales, 50 μm .



Supplementary Figure 8. (A) Immunohistochemistry of TRPV1 and GRP in the spinal cord dorsal horn of WT and *Tlr3*^{-/-} mice. Note that the intensity of TRPV1+ and GRP+ signaling is reduced in *Tlr3*^{-/-} mice. Scales, 50 μ m. **(B)** Quantification of the intensity of TRPV1, GRP, CGRP, and NF-200 staining in the superficial dorsal horn. Note that CGRP and NF200 staining does not change in *Tlr3*^{-/-} mice. * $P < 0.05$, compared to WT mice. 2-tailed Student's *t* test, $n = 4$ mice. **(C)** Intrathecal injection of GRP (GRP₁₈₋₂₇, 1 nmol) induces comparable scratching responses in WT and *Tlr3*^{-/-} mice. $P > 0.05$, 2-tailed Student's *t* test, $n = 8$ mice.



Supplementary Figure 9. (A) Traces of sEPSCs in the lamina II neurons of the spinal cord slices from *Trpv1^{-/-}* mice following treatment of PIC (100 ng/ml) and mustard oil (100 nM). Note increases in sEPSC frequency after PIC and mustard oil treatment. (B) Quantification of sEPSC frequency and amplitude before and after PIC treatment in WT and *Trpv1^{-/-}* mice. Note that PIC increases the frequency but not amplitude of sEPSC in both WT and *Trpv1^{-/-}* mice, despite a decrease in basal sEPSC frequency in the KO mice. n=5 neurons. * $P < 0.05$, compared with WT pretreatment baseline.



Supplemental Figure 10. *Tlr3*^{-/-} mice exhibit normal skin morphology and expression of mast cell markers. (A) H&E staining showing the morphology of hair follicles in the hairy skins of WT and *Tlr3*^{-/-} mice. Scales, 100 μm. (B) Quantification of the number of hair follicles in the hairy skins of WT and *Tlr3*^{-/-} mice. (C) Quantification of the percentage of hair follicles at different growth cycles in WT and *Tlr3*^{-/-} mice. (D) Toluidine blue (TB) staining showing mast cells in the hairy skins. Scales, 50 μm. (E) Quantification of the number of mast cells in the skins of WT and *Tlr3*^{-/-} mice. (F) Histamine content in the skins of WT and *Tlr3*^{-/-} mice, as revealed by ELISA analysis. (G) Histamine released induced by compound 48/80 (100 μg/ml, 30 min) in organ cultures of skins from WT and *Tlr3*^{-/-} mice. (H) Quantitative RT-PCR showing the expression of mast cell markers: mouse tryptase (TPSAB1), chymases (CMA1), and c-Kit (CD117), as well as the expression of NGF in WT and *Tlr3*^{-/-} mice. *P*>0.05, 2-tailed Student's *t* test, n=4 mice in all the cases.